12 Mar 1991, 10:30 am - 12:00 pm

Modelling the Deformation of Sand during Cyclic Rotation of Principal Stress Directions

Marte Gutierrez
Norwegian Geotechnical Institute, Oslo, Norway

Kenji Ishihara
University of Tokyo, Japan

Ikuo Towhata
University of Tokyo, Japan

Proceedings: Second International Conference on Recent Advances in Geotechnical Earthquake Engineering and Soil Dynamics, March 11-15, 1991, St. Louis, Missouri, Paper No. 1.3

Modelling the Deformation of Sand during Cyclic Rotation of Principal Stress Directions

Marte Gutierrez
Norwegian Geotechnical Institute, P.O. Box 40, Tåsen, N-0801 Oslo 8, Norway

Kenji Ishihara and Ikuo Towhata
Department of Civil Engineering, University of Tokyo, Bunkyo-ku, Tokyo 113, Japan

SYNOPSIS

The paper presents an elastoplastic constitutive model for the deformation of sand during cyclic rotation of principal stress directions. The model employs a plastic potential theory that allows for the dependency of flow on the stress increment direction and a stress-dilatancy relation incorporating the effects of noncoaxiality. The continuous plastic deformation of sand during principal stress rotation at constant shear stress level is allowed for in the model by using a small elastic area in the stress space. The effects of cyclic stress history is modelled by using discrete surfaces of equal hardening modulus which are allowed to move with the stress point during loading. Additionally, the plastic hardening modulus is allowed to stiffen during cyclic loading depending on the amount of accumulated plastic normalized work. The model is used to simulate the deformations in the hollow cylindrical specimen subjected to several cycles of principal stress rotations. The model is shown to be capable of satisfactorily predicting the response of sand during cycles of principal stress rotations.

INTRODUCTION

Actual in-situ stress paths such as those caused by earthquakes, vehicular traffic and sea waves invariably involve rotation of principal stress directions. While there have been numerous studies showing the important effects of principal stress rotation on the behavior of soils (e.g., Arthur et al., 1980; Ishihara and Towhata, 1983), there have been very few attempts to model the deformation of soils during principal stress rotation. This can be due to the fact that two characteristics of the response of sand during principal stress rotation, namely, noncoaxiality and the dependency of flow on the stress increment direction, pose severe difficulties in the formulation of constitutive models. In fact, these two factors are not allowed for in almost all of the currently available constitutive models for soils.

The authors have embarked on a series of tests using the hollow cylindrical apparatus to determine the behavior of sand during principal stress rotation. The results of the experiments have been used as basis in the formulation of an elastoplastic constitutive model capable of simulating the response of sand subjected to loading conditions with changing directions of the principal stresses.

Further details of the model can be obtained in Gutierrez et al. (1989a; 1990) where it has been shown to satisfactorily capture the response of sand during "monotonic" rotation of principal stress directions. This paper presents the extensions to the formulation to enable it to model sand deformation during cyclic rotation of principal stress directions. Comparisons of the model predictions with experimental results demonstrate the adequacy of the proposed model.

For simplicity, a two-dimensional, plane strain representation is used but extension to three dimensions is possible. The model assumes that b-value ($b=(\sigma_2-\sigma_3)/(\sigma_1-\sigma_3)$) is constant and equal to 0.5 for plane strain condition. Strictly, b-value varies during loading in plane strain condition and a three-dimensional formulation is required, but the assumption of a constant b-value results in enormous savings in computational efforts.

STRESS AND STRAIN INCREMENT REPRESENTATION

For plane strain condition, it is sufficient to represent the state of stress in the sand in the $p-X-Y$ stress space, Figure 1, where

$$p=\frac{1}{2}(\sigma_x+\sigma_y) \quad (1)$$

$$X=\frac{1}{2}(\sigma_y-\sigma_x) \quad (2)$$

$$Y=\sigma_{xy} \quad (3)$$

In the $X-Y$ stress plane, a vector from the origin has a length equal to the shear stress

$$q=\sqrt{\left(\frac{\sigma_x+\sigma_y}{2}\right)^2+\sigma_{xy}^2} \quad (4)$$

and makes an angle equal to 2α from the X-axis. α is the angle the major principal stress σ_1 makes with the y-axis. This angle is defined as

$$\tan 2\alpha=\frac{2\sigma_{xy}}{\sigma_y-\sigma_x} \quad (5)$$

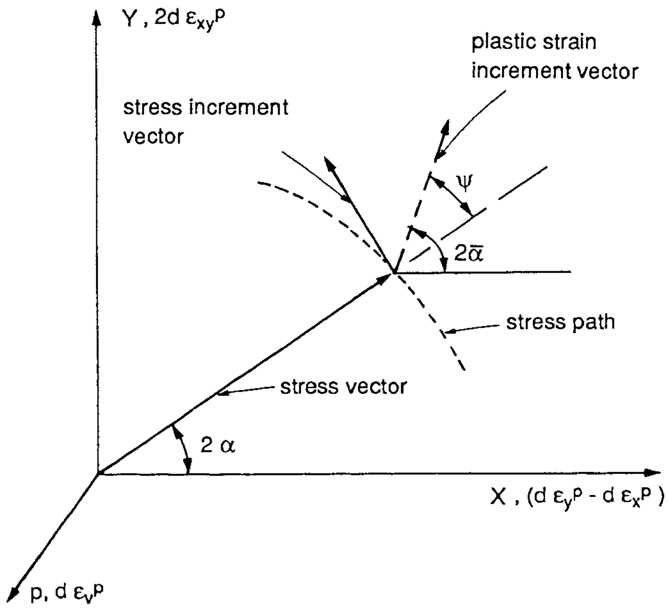

Figure 1. Stress and strain increment representation in the $p-X-Y$ stress space.

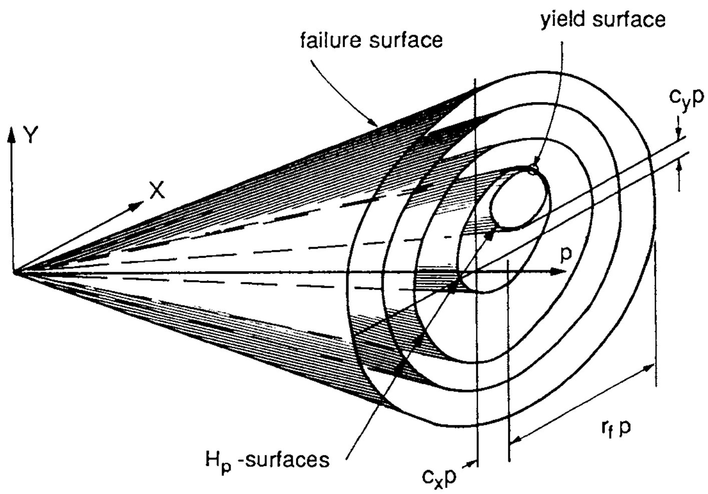

Figure 2. Failure, yield and plastic hardening modulus surfaces in the $p-X-Y$ stress space

The strain increments can also be sufficiently represented by superimposing the plastic strain increment components $d\epsilon_v^p$, $(d\epsilon_y^p - d\epsilon_x^p)$ and $2d\epsilon_{xy}^p$ on the stress path in the $p-X-Y$ stress space, Figure 1. $d\epsilon_v^p$ is the plastic volumetric strain increment

$$d\epsilon_v^p = d\epsilon_x^p + d\epsilon_y^p \tag{6}$$

A plastic strain increment vector in the $X-Y$ plane has a length equal to the plastic shear strain increment

$$d\bar{\epsilon}^p = \sqrt{(d\epsilon_y^p - d\epsilon_x^p)^2 + 4d\epsilon_{xy}^{p2}} \tag{7}$$

and makes an angle equal to $\bar{\alpha}$ from the X-axis. $\bar{\alpha}$ is the angle the major principal strain increment $d\epsilon_1^p$ makes with the y-axis and is defined as

$$\tan 2\bar{\alpha} = \frac{2d\epsilon_{xy}^p}{d\epsilon_y^p - d\epsilon_x^p} \tag{8}$$

FAILURE SURFACE

From the results of a series of monotonic tests along different directions α of the major principal stress σ_1, it was found that the anisotropic strength of sand can be modelled by a failure surface of the form, Figure 2,

$$F = \sqrt{(X - c_x p)^2 + (Y - c_y p)^2} - r_f p \tag{9}$$

The failure surface appears as a cone in the $p-X-Y$ stress space and has a circular section in the $X-Y$ plane with center at $(c_x p, c_y p)$ and a radius $r_f p$. For isotropic sand $r_f = \sin\phi_f$, where ϕ_f is the angle of friction at failure.

The parameters c_x and c_y reflect the anisotropic strength of sand. In the case of isotropic response, both c_x and c_y are equal to zero and the axis of the conical failure surface coincides with the p-axis. In the case of orthotropic response, i.e., the same response for positive or negative σ_{xy}, c_y is equal to zero.

Experimental results indicate that only initial anisotropy affects the strength of sand and that induced anisotropy changes this initially anisotropic strength only very slightly. The parameters c_x and c_y may therefore be considered as essentially constant and practically unchanged during loading.

On the other hand, it was found that the relative density of the sand has a profound effect on its strength. Consequently, the formulation allows the failure surface to expand or contract depending on the amount of accumulated plastic volumetric strain. The following equation based on a formulation by Mogami (1965) was found to be adequate

$$r_f = \frac{r_{fo}}{1 - \epsilon_v^p} \tag{10}$$

r_{fo} is the value of r_f at a reference void ratio e_o.

FLOW RULE

Based on the results of an extensive series of tests (Gutierrez et al., 1989b), the flow of sand during loadings involving principal stress rotation is represented by the plastic potential formulation shown in Figure 3. In the $X-Y$ plane, the direction of the principal plastic strain increment $d\epsilon_1^p$ is evaluated as the normal to the failure surface at the point (X^c,Y^c), which is referred to as the conjugate stress point. (X^c,Y^c) is the intersection of the failure surface and the stress increment vector extended. This flow rule is based on experimental results showing non-uniqueness in flow or dependency of the plastic strain increment direction on the stress increment direction in sand during principal stress rotation. Such type of response can not be handled by usual plastic potential formulations.

From Figure 3,

$$d\epsilon_y^p - d\epsilon_x^p = d\lambda\left(\frac{\partial F}{\partial X}\right)_{X=X^c, Y=Y^c} = d\lambda\left(\frac{X^c - c_x p}{r_f p}\right) \quad (11)$$

$$d\epsilon_{xy}^p = d\lambda\left(\frac{\partial F}{\partial Y}\right)_{X=X^c, Y=Y^c} = d\lambda\left(\frac{Y^c - c_y p}{2r_f p}\right) \quad (12)$$

where $d\lambda$ is a constant that can be obtained from Prager's consistency condition, giving the magnitudes of the plastic strain increments. The magnitude of the plastic shear strain increment can now be calculated by substituting Eqs. (11) and (12) in Eq. (7)

$$d\bar{\epsilon}^p = d\lambda \quad (13)$$

while the direction of $d\epsilon_1^p$ can be solved as

$$\tan 2\bar{\alpha} = \frac{Y^c - c_y p}{X^c - c_x p} \quad (14)$$

To calculate the plastic volumetric strain increment, a stress-dilatancy relation taking into account the noncoaxiality or non-coincidence of the principal stress and principal plastic strain increment directions is used (Gutierrez, et al., 1988). The stress-dilatancy relation is given as

$$\frac{d\epsilon_v^p}{d\bar{\epsilon}^p} = \sin\phi_c - \frac{q}{p}\cos 2\psi \quad (15)$$

where

$$\psi = |\alpha - \bar{\alpha}| \quad (16)$$

is the angle of noncoaxiality, Figure 1, and ϕ_c is the angle of friction at zero dilatancy. Noncoaxiality is another prominent feature of sand response during principal stress rotation which can not be handled by usual plasticity formulations. Using Eq. (13), the plastic volumetric strain increment can now be expressed as

$$d\epsilon_v^p = (d\epsilon_x^p + d\epsilon_y^p) = d\lambda\left(\sin\phi_c - \frac{q}{p}\cos 2\psi\right) \quad (17)$$

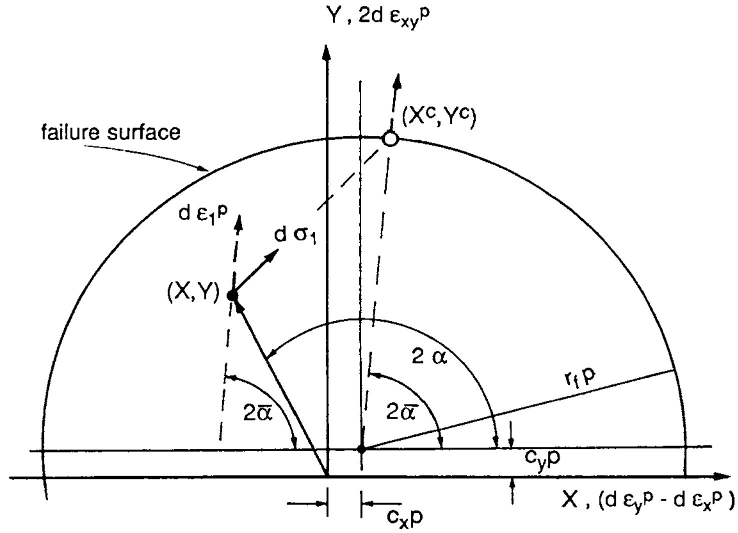

Figure 3. Plastic potential formulation in the $X-Y$ stress plane.

By using Eqs. (11), (12) and (17), the complete flow rule can be easily derived as

$$d\epsilon_x^p = \frac{d\lambda}{2}\left\{\left(\sin\phi_c - \frac{q}{p}\cos 2\psi\right) - \left(\frac{X^c - c_x p}{r_f p}\right)\right\} \quad (18)$$

$$d\epsilon_y^p = \frac{d\lambda}{2}\left\{\left(\sin\phi_c - \frac{q}{p}\cos 2\psi\right) + \left(\frac{X^c - c_x p}{r_f p}\right)\right\} \quad (19)$$

$$d\epsilon_{xy}^p = \frac{d\lambda}{2}\left\{\frac{Y^c - c_y p}{r_f p}\right\} \quad (20)$$

YIELD SURFACE AND HARDENING FUNCTIONS

The scalar quantity $d\lambda$ can be obtained from the consistency condition which gives

$$d\lambda = \frac{1}{H_p}\left(\frac{\partial f}{\partial \sigma_{kl}}\sigma_{kl}\right)$$
$$= \frac{1}{H_p}\left(\frac{\partial f}{\partial \sigma_x}d\sigma_x + \frac{\partial f}{\partial \sigma_y}d\sigma_y + 2\frac{\partial f}{\partial \sigma_{xy}}d\sigma_{xy}\right) \quad (21)$$

or by using the chain rule of differentiation

$$d\lambda = \frac{1}{H_p}\left\{\left(\frac{\partial f}{\partial p}\frac{\partial p}{\partial \sigma_x} + \frac{\partial f}{\partial X}\frac{\partial X}{\partial \sigma_x}\right)d\sigma_x + \left(\frac{\partial f}{\partial p}\frac{\partial p}{\partial \sigma_y} + \frac{\partial f}{\partial X}\frac{\partial X}{\partial \sigma_y}\right)d\sigma_y + 2\left(\frac{\partial f}{\partial Y}\frac{\partial Y}{\partial \sigma_{xy}}\right)d\sigma_{xy}\right\} \quad (22)$$

where H_p is the plastic hardening modulus and f is the yield function, which now needs to be formulated. It is to be noted that as an additional condition, plastic strains as given in Eq. (21) are possible only if the yield criteria is satisfied, i.e., $f=0$.

To allow for the continuous plastic deformation of sand during principal stress rotation with the shear stress level maintained constant, a yield surface with a very small elastic area in the $X-Y$ plane is used. The proposed yield surface is a straight line passing through the origin of the $p-X-Y$ stress space. With this yield surface the criteria $f=0$ is always satisfied for any stress increment direction in the $X-Y$ stress plane and hence, plastic strains always occur. However, with a small elastic area in the $X-Y$ plane, the normal to the yield surface $\partial f/\partial X$ and $\partial f/\partial Y$ cannot be determined.

Experimental results by the authors indicate that flow in the $X-Y$ plane can be taken as associative, i.e, the plastic strain increment direction and the normal to the yield surface are the same. Thus, the normal to the yield surface can be obtained by simply replacing the derivatives $\partial f/\partial X$ and $\partial f/\partial Y$ with the derivatives giving the normals to the failure surface at the conjugate stress point (X^c, Y^c), i.e.,

$$\frac{\partial f}{\partial X} = \left.\frac{\partial F}{\partial X}\right|_{X=X^c, Y=Y^c} = \frac{X^c - c_x p}{r_f p} \qquad (23)$$

$$\frac{\partial f}{\partial Y} = \left.\frac{\partial F}{\partial Y}\right|_{X=X^c, Y=Y^c} = \frac{Y^c - c_y p}{2 r_f p} \qquad (24)$$

Since the yield surface is a straight line in the $p-X-Y$ stress space, $\partial f/\partial p = -q/p$. $d\lambda$ can now be obtained by noting that $\partial p/\partial \sigma_x = 1/2$, $\partial p/\partial \sigma_y = 1/2$, $\partial X/\partial \sigma_x = -1/2$, $\partial X/\partial \sigma_y = 1/2$ and $\partial Y/\partial \sigma_{xy} = 1$.

$$d\lambda = \frac{1}{H_p}\left\{\frac{1}{2}\left(-\frac{q}{p} - \frac{X^c - c_x p}{r_f p}\right)d\sigma_x + \frac{1}{2}\left(-\frac{q}{p} + \frac{X^c - c_x p}{r_f p}\right)d\sigma_y + \left(\frac{Y^c - c_y p}{r_f p}\right)d\sigma_{xy}\right\} \qquad (25)$$

The variation of the plastic hardening modulus H_p during loading is modelled by using the concept of a field of nesting contours of hardening surfaces of equal plastic hardening modulus, very similar to the nesting yield surfaces formulation (Mroz, 1967; Prevost and Høeg, 1975). The H_p-surfaces are circular cones initially concentric with the failure surface, Figure 2. Upon contact, these surfaces are to be translated by the stress point. The movement of the H_p-surfaces are prescribed in a manner that insures their non-intersection.

To model the effects of both shear stress level and cyclic loading history, the plastic hardening modulus is defined to be a product of two functions: a backbone curve H_1 reflecting the effect of shear stress level and a monotonically increasing function H_2 which manifests the stiffening of the plastic hardening modulus during loading. The plastic hardening modulus for a plastic hardening surface of size r_i is calculated as

$$H_p = H_1 H_2 \qquad (26)$$

where

$$H_1 = G_p p\left(\frac{p}{p_a}\right)^m\left(1 - \frac{r_i}{r_f}\right)^2 \qquad (27)$$

$$H_2 = \exp(h\Omega^p) \qquad (28)$$

where G_p is the initial plastic shear modulus. m is a material parameter modelling the dependency of the plastic hardening modulus on the mean stress and h models the stiffening of H_p as a function of the accumulated normalized plastic work Ω^p defined as

$$\Omega^p = \int\left(d\epsilon_v^p + \frac{q}{p} d\bar{\epsilon}^p \cos 2\psi\right) \qquad (29)$$

Equations (26) to (28) indicate a response which at the start of cyclic loading is almost purely plastic. As Ω^p increases, the plastic hardening modulus starts to increase causing the plastic deformation to decrease until the final stage when H_p becomes very large. At this stage, the soil "shakesdown" and starts to behave like an elastic material.

In addition to the plastic strains, the elastic strains need to be determined and added to the plastic ones. The elastic strains are assumed to be isotropic and all anisotropic response comes from plasticity. Hence, only two elastic parameters are needed to calculate the elastic strains. The elastic parameters are given by a pressure-dependent Young's modulus, E, and a constant Poisson's ratio, ν. The same parameter m which models the pressure-dependency of the plastic hardening modulus is used to reflect the pressure-dependency of E.

For stress-controlled loading conditions, the above equations constitute the complete incremental formulation and implementation of the model is quite straightforward. However, the application of the model to strain-controlled loading conditions is much more complicated. This is because the stress increments are now the unknowns and at the same time the formulation requires the direction of the principal stress increment. Implementation of the model in strain-controlled situations would therefore require iterations within an increment of loading.

COMPARISONS WITH EXPERIMENTAL RESULTS

The model has been used to simulate the experimental results of Miura et al. (1986) on hollow cylindrical tests of dense Toyoura sand with a relative density D_r=95%. The tests were conducted at a constant b-value of 0.5 and mean stress of p=98.1 kPa. Comparisons were made with tests involving several cycles of pure rotation of principal stress directions at a constant angle of friction of ϕ=30°. The material parameters used in the simulation are given in Table 1.

Table 1. Model parameters for Toyoura sand

Elastic parameters	
E	300 MPa
ν	0.2
m	0.5
Hardening parameters	
G_{po}	95 MPa
h	15
Strength parameters	
r_f	0.79
c_x	0.08
c_y	0
Dilatancy parameter	
ϕ_c	20.5°

Figure 4 shows the predicted and measured strain components ϵ_x, ϵ_y and ϵ_{xy} for the first and seventh cycles of principal stress rotation. The predicted and measured strain components agree well specially for the first cycle. The tendency of the strain components to flatten out after several cycles of rotation is remarkably represented by the model.

Figure 5 compares the predicted and measured total strain increments superimposed on the stress path on the $X-Y$ plane for the same cycles of rotation. Again, there is a good agreement between the predicted and experimental results. The model captures adequately the increasing deviation of the total principal strain increment direction from the principal stress direction due to the increasing predominance of the elastic strain components viz-a-viz the plastic strains.

REFERENCES

Arthur, J.R.F., Chua, K.S., Dunstan, T. and Rodriguez del C.J.I. (1980), "Principal Stress Rotation: A Missing Parameter," Journal of Geotechnical Engineering, ASCE, vol. 106, GT4, pp. 418-433

Gutierrez, M., Ishihara, K., Towhata, I. and Hyodo, H. (1988), "Stress-dilatancy of Sand Subjected to Rotation of Principal Stress Directions", Proc. 23rd Conf. of JSSMFE

Gutierrez, M., Ishihara, K. and Towhata, I. (1989a), "A Plasticity Model for the Deformation of Sand During Rotation of Principal Stress Directions", Proc. 3rd Intl. Symp. on Num. Meth. in Geomechanics (NUMOG III), Niagara Falls

Gutierrez, M., Ishihara, K. and Towhata, I. (1989b), "A Plastic Potential Theory for the Non-unique Flow of Sand During Principal Stress Rotation", Proc. 7th Intl. Conf. on Numerical Methods in Engineering, Laussane

Gutierrez, M., Ishihara, K. and Towhata, I. (1990), "A Plasticity Model for the Simple Shear Deformation of Sand", Proc. Intl. Conf on Numerical Methods in Engineering; Theory and Applications (NUMETA 90), Wales, Swansea.

Ishihara, K. and Towhata, I. (1983), "Sand Response to Cyclic Rotation of Principal Stress Directions as Induced by Wave Loads," Soils and Foundations, vol. 23, no. 4, pp. 11-26

Miura, K., Miura, S. and Toki, S. (1986), "Deformation Behaviour of Anisotropic Sand Under Principal Axes Rotation", Soils and Foundations, vol. 26, no. 1, pp. 36-52

Mogami, T. (1965), "A Statistical Approach to the Mechanics of Granular Material" Soils and Foundation, vol. 5, no. 5., pp. 23-36

Mroz, Z. (1967), "On the Description of Anisotropic Workhardening", Journal of the Mechanics and Physics of Solids, vol. 15, pp. 163-175.

Prevost, J. H. and Høeg, K. (1975), "Mathematical Model for Static and Cyclic Undrained Clay Behaviour," Norwegian Geotechnical Institute Report Nos. 52412-1, 52412-2

ACKNOWLEDGMENTS

The first author acknowledges the financial support of the Japanese Ministry of Education (Monbusho) and the Royal Norwegian Council for Scientific and Industrial Research (NTNF).

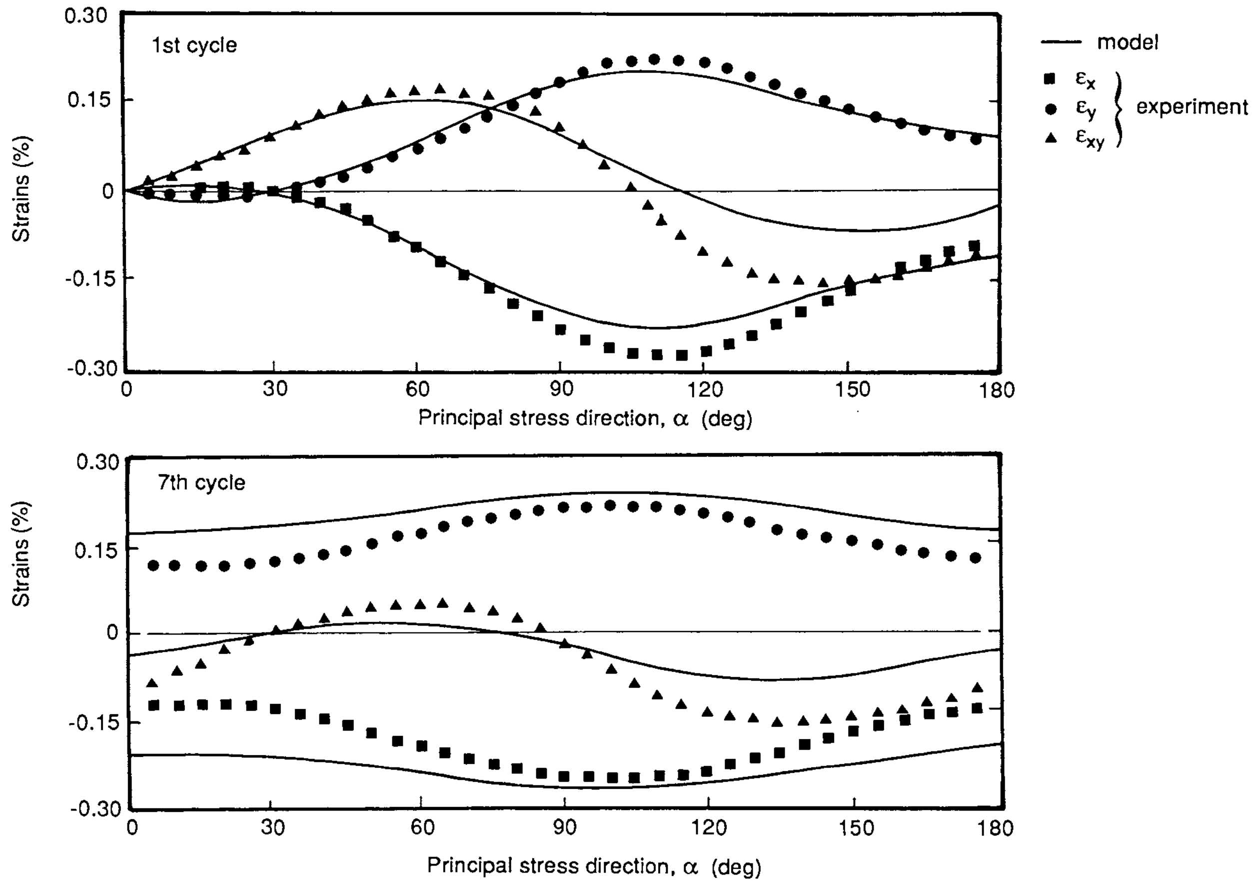

Figure 4. Comparisons of predicted and measured strains during seven cycles of principal stress rotation.

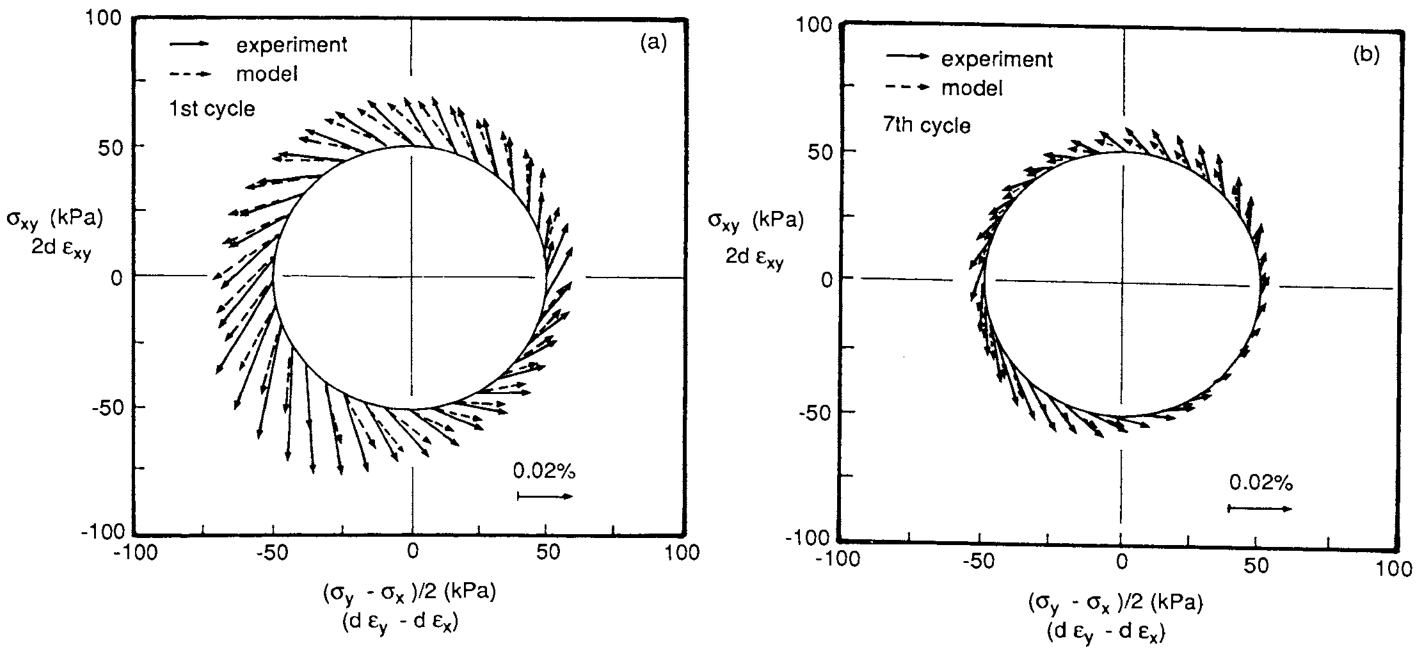

Figure 5. Comparisons of predicted and measured strain increments during seven cycles of principal stress rotation.